European Journal of Neuroscience, Vol. 18, pp. 2925–2934, 2003

The immunocytochemical localization of connexin 36 at rod and cone gap junctions in the guinea pig retina

Eun-Jin Lee,* Jung-Won Han,* Hyun-Ju Kim, In-Beom Kim, Mun-Yong Lee, Su-Ja Oh, Jin-Woong Chung and Myung-Hoon Chun
Department of Anatomy, College of Medicine, The Catholic University of Korea, Seoul 137-701, Korea

Keywords: cone cell, connexin 36, gap junction, immunocytochemistry, rod cell

Abstract

Connexin 36 (Cx36) is a channel-forming protein found in the membranes of apposed cells, forming the hexameric hemichannels of intercellular gap junction channels. It localizes to certain neurons in various regions of the brain including the retina. We characterized the expression pattern of neuronal Cx36 in the guinea pig retina by immunocytochemistry using specific antisera against Cx36 and green/red cone opsin or recoverin. Strong Cx36 immunoreactivity was visible in the ON sublamina of the inner plexiform layer and in the outer plexiform layer, as punctate labelling patterns. Double-labelling experiments with antibody directed against Cx36 and green/red cone opsin or recoverin showed that strong clustered Cx36 immunoreactivity localized to the axon terminals of cone or close to rod photoreceptors. By electron microscopy, Cx36 immunoreactivity was visible in the gap junctions as well as in the cytoplasmic matrices of both sides of cone photoreceptors. In the gap junctions between cone and rod photoreceptors, Cx36 immunoreactivity was only visible in the cytoplasmic matrices of cone photoreceptors. These results clearly indicate that Cx36 forms homologous gap junctions between neighbouring cone photoreceptors, and forms heterologous gap junctions between cone and rod photoreceptors in guinea pig retina. This focal location of Cx36 at the terminals of the photoreceptor suggests that rod photoreceptors can transmit rod signals to the pedicle of a neighbouring cone photoreceptor via Cx36, and that the cone in turn signals to corresponding ganglion cells via ON and OFF cone bipolar cells.

Introduction

Gap junctions are specialized membrane regions consisting of hexameric assemblies of proteins (connexins) in the apposed membranes of adjacent cells. The passage of ions and small molecules (<1 kDa) through gap junction channels results in the metabolic and electrical coupling of cells (Bruzzone *et al*., 1996; Goodenough *et al*., 1996). Electronic coupling mediated by gap junctions has been proposed as being responsible for the synchronization of signals and neuronal adaptation in various brain regions, including the retina (Sterling, 1995; Galarreta & Hestrin, 1999; Traub *et al*., 1999; Tamas *et al*., 2000; Weiler *et al*., 2000). Connexins are encoded by a large multigene family: 15 different forms have been identified so far (Beyer *et al*., 1990; Willecke *et al*., 1991; Haefliger *et al*., 1992; Bruzzone *et al*., 1996; Dahl *et al*., 1996).

In the mammalian retina, a number of different connexins are expressed in astrocytes (Dermietzel & Spray, 1998), Müller cells, type AII amacrine cells and pigment epithelial cells, as well as photoreceptor cells (Janssen-Bienhold *et al*., 1998; Feigenspan *et al*., 2001; Guldenagel *et al*., 2001; Mills *et al*., 2001; Umino & Saito, 2002; Zahs *et al*., 2003). These connexins play important roles in the processing of visual information in the retina, by regulating the sensitivity and receptive field organization of retinal neurons, and through the photic modulation of gap junction conductance (Dong & McReynolds, 1991; Weiler & Akopian, 1992). Studies using electrical recording and dye coupling have shown that both homologous and heterologous coupling exist in the retina (Vaney, 1999). Connexin 36 (Cx36) is also involved in both homologous gap junctions between neighbouring AII amacrine cells, and heterologous gap junctions between AII amacrine cells and ON cone bipolar cells in mouse, rat and rabbit retinas (Feigenspan *et al*., 2001; Guldenagel *et al*., 2001; Mills *et al*., 2001). Rod signals generated under scotopic light conditions are passed into the cone system through these heterologous junctions (Mills *et al*., 2001). Rod signals may also travel via gap junctions to cones, and from there to the ON and OFF cone bipolar cells. Electrical coupling connections between rod and cone photoreceptors in the vertebrate retina have been observed both physiologically (Nelson, 1977; Schneeweis & Schnapf, 1995) and anatomically (Raviola & Gilula, 1973, 1975; Smith *et al*., 1986). Deans *et al*. (2002) suggested that all pathways from rods to ON and OFF ganglion cells require Cx36 gap junctions for signal transmission in the mouse retina.

Cx36 immunoreactivity has been reported in the outer plexiform layer (OPL) of the rat retina (Feigenspan *et al*., 2001). In addition, Deans *et al*. (2002) have suggested that Cx36 could be expressed in the rod photoreceptors. However, the direct localization of Cx36 responsible for gap junctions between rod and cone photoreceptors has not been reported in any mammalian retina examined so far. We therefore investigated the expression and cellular localization of Cx36 in the guinea pig retina by immunocytochemistry using antibodies against Cx36 or Cx35/36.

Materials and methods

Tissue preparation

Five adult guinea pigs of either sex were used. Three adult Sprague–Dawley rats were also used as controls. The animals were treated

Correspondence: Dr M.-H. Chun, as above.
E-mail: mhchun@catholic.ac.kr

*E.-J.L. and J.-W.H. contributed equally to this work.

Received 19 April 2003, revised 24 September 2003, accepted 26 September 2003

doi:10.1046/j.1460-9568.2003.03049.x

according to the regulations of the Catholic Ethics Committee of the Catholic University of Korea, Seoul, which conforms to all National Institute of Health guidelines. The animals were killed by an intraperitoneal overdose of 4% chloral hydrate (4 mL/100 g body weight), and the eyes were enucleated. The anterior segments of the eyeballs were removed. For Western blot analysis, retinal tissues were quickly dissected on an ice-cold plate, frozen on dry ice, and stored at −70 °C. For immunocytochemistry, the eyecups were fixed by immersion in fixative [4% paraformaldehyde/0.2% picric acid in 0.1 M phosphate buffer (PB, pH 7.4)] for 2–3 h. Following fixation, the retinas were carefully dissected and transferred to 30% sucrose in PB, for 24 h at 4 °C. They were then frozen in liquid nitrogen, thawed, and rinsed in 0.01 M phosphate-buffered saline (PBS, pH 7.4).

Western blot analysis

Western blot analysis was performed on the retinal extracts, which were homogenized in 10 vol. of 20 mM Tris–HCl, pH 7.4, 150 mM NaCl, 1 mM EDTA, 1% Triton X-100, 0.5% sodium deoxycholate, 0.1% SDS, 0.02% sodium azide, 1 mM phenyl methyl sulphoryl fluoride, and 5 μg/mL leupeptin. Aliquots of tissue samples corresponding to 10 μg of total protein were heated at 100 °C for 10 min with an equivalent volume of 2 × sample buffer (containing 4% SDS and 10% mercaptoethanol) and loaded onto 10% polyacrylamide gels. The proteins were electrotransferred to a nitrocellulose membrane in Tris–glycine–methanol buffer. The membrane was blocked for 1 h at room temperature in a blocking solution containing 5% non-fat dry milk, 0.05% Tween-20 and PBS (pH 7.4). The membrane was then incubated for 15 h at 4 °C with a rabbit polyclonal antibody against Cx36 (Zymed Laboratories, San Francisco, CA, USA; dilution 1 : 1000) or a mouse monoclonal antibody directed against Cx35/36 (Chemicon International, Temecula, CA, USA; dilution 1 : 1000) in blocking solution. The membrane was rinsed with 0.05% Tween-20 in PBS for three washes of 10 min and incubated for 1 h at room temperature in a 1 : 2000 dilution of peroxidase-conjugated goat anti-mouse or anti-rabbit IgG antibody (Jackson Immuno Laboratories, West Grove, PA, USA). The blot was washed three times each for 10 min and then processed for analysis using an Enhanced Chemiluminescence detection kit (Amersham, Arlington Heights, IL, USA).

Immunocytochemistry

For immunocytochemistry, 50-μm-thick vibratome sections were incubated in 10% normal goat serum and 1% Triton X-100 in PBS for 1 h at room temperature to block non-specific binding sites. The sections were then incubated overnight at 4 °C with a rabbit polyclonal antibody directed against Cx36 (Zymed; dilution 1 : 1000) or a mouse monoclonal antibody directed against Cx35/36 (Chemicon; dilution 1 : 1000) in PBS containing 0.5% Triton X-100. Retinas were washed in PBS for 45 min (3 × 15 min), and incubated for 2 h in fluorescein isothiocyanate (FITC)-conjugated affinity-purified anti-rabbit or anti-mouse IgG (Jackson Immuno Laboratories; dilution 1 : 100) and in peroxidase-conjugated goat anti-rabbit IgG (Jackson Immuno Laboratories; dilution 1 : 100) at room temperature. The sections treated with FITC-conjugated antibodies were washed for 30 min with 0.1 M PB and cover-slipped with 10% glycerol in 0.1 M PB. Images were imported into Adobe Photoshop version 5.5 (Adobe Systems, Mountain View, CA, USA). For presentation, all manipulations (brightness and contrast only) were carried out equally on all images. The sections treated with peroxidase-conjugated goat anti-rabbit IgG were washed in TB, and then incubated in 0.05% 3,3′ diaminobenzidine (DAB) solution containing 0.01% H_2O_2. The reaction was monitored using a low-power microscope, and was stopped by replacing the DAB and H_2O_2 solution with TB.

Double-immunocytochemistry

For double-label studies, sections were incubated overnight in a mixture of anti-Cx35/36 antibody (Chemicon; dilution 1 : 1000) or anti-Cx36 antibody (Zymed Laboratories; dilution 1 : 1000) with the following antibodies: rabbit polyclonal anti-green/red cone opsin (kindly provided by Dr J. Nathans, Johns Hopkins University, School of Medicine; diluted to 1 : 4000); rabbit polyclonal anti-recoverin (kindly provided by Dr K.W. Koch, Institut für Biologische Informationsverarbeitung, Jülich, Germany; dilution 1 : 1000); and monoclonal anti-calbindin (Sigma, St. Louis, CA, USA; dilution 1 : 1000), all in 0.5% Triton X-100 in 0.1 M PBS at 4 °C. Sections were rinsed for 30 min with 0.1 M PBS, and incubated in FITC-conjugated affinity-purified anti-mouse or anti-rabbit IgG (Jackson Immuno Laboratories; diluted to 1 : 100) and Cy3-conjugated anti-rabbit or anti-mouse IgG (Jackson Immuno Laboratories; diluted to 1 : 500) for 1–2 h at room temperature. Sections were washed for 30 min with 0.1 M PB and cover-slipped with 10% glycerol in 0.1 M PB. To ensure that the secondary antibody had not cross-reacted with the inappropriate primary antibody, some sections were incubated in rabbit

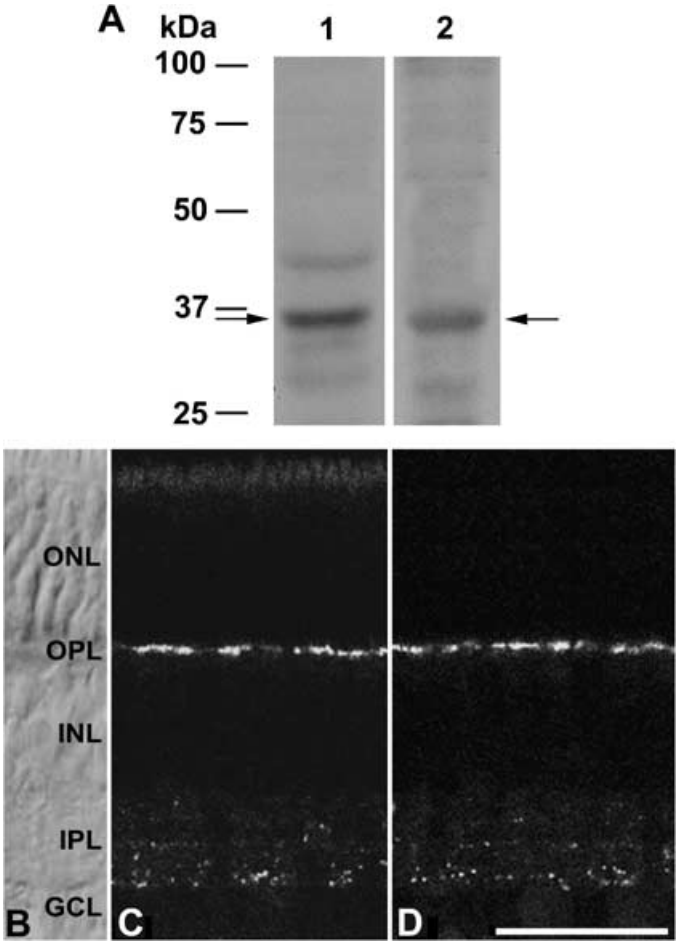

FIG. 1. (A) Western blot analysis of Cx36 (lane 1) and Cx35/36 (lane 2) in the guinea pig retina. Positions and molecular weights (in kDa) are indicated by arrows. (B) Light micrograph taken from a vertical vibratome section (50 μm) immunostained with pre-immune serum. No immunostaining is seen. Fluorescent micrographs taken from a vertical vibratome section (50 μm) processed for Cx36 (C) and Cx35/36 (D) immunoreactivities in the guinea pig retina. Cx36- or Cx35/36-immunoreactive puncta are visible in the ON sublamina of the IPL and less so in the OFF sublamina. In the OPL, the labelled puncta are also visible. Note the faint non-specific labelling in the inner segment in C. GCL, ganglion cell layer; INL, inner nuclear layer; IPL, inner plexiform layer; ONL, outer nuclear layer; OPL, outer plexiform layer. Scale bar, 50 μm.

polyclonal primary antibody followed by anti-mouse secondary antibody, while other sections were incubated in mouse primary antibody followed by anti-rabbit secondary antibody. These sections did not show any immunostaining.

Cell dissociation

For dissociation of the retina, eyes were enucleated from adult guinea pigs. After removal of the cornea, lens and vitreous body, each was transferred to a solution containing 20 U/mL papain (Worthington, Freehold, NJ, USA) and 200 U/mL DNase I (Sigma) in Earle's Balanced Salt Solution (Sigma) for 15 min. Following this enzyme treatment, the retina was rinsed two–three times with Earle's Balanced Salt Solution and shaken gently until the tissue dissociated. The cells were placed on a lectin (Sigma)-coated coverslip in a Petri dish filled with Ringer's solution. The cells were allowed to settle on the coverslip for at least 30 min at 36 °C in an atmosphere of 5% CO_2 and 95% air. The cells were then washed in PBS and fixed in 4% paraformaldehyde for 20 min and processed for fluorescence immunocytochemistry as described above.

Confocal laser scanning microscopy

Sections were analysed using a Bio-Rad Radiance Plus confocal scanning microscope (Bio-Rad, Hemel Hempstead, UK), installed on a Nikon Eclipse E600 fluorescence microscope (Nikon, Tokyo, Japan). FITC and Cy3 signals were always detected separately. The FITC labelling was excited using the 488-nm line of the Argon ion laser and detected after passing an HQ513/30 (Bio-Rad) emission filter. For detection of the Cy3 signal, the 543-nm line of the green HeNe laser was used in combination with the 605/32 (Bio-Rad) emission filter. Images were imported into Adobe Photoshop version 5.5 (Adobe Systems) and printed on photographic quality paper (Seiko Epson Corporation, Japan). For presentation, all manipulations (brightness and contrast only) were carried out equally for all images.

Electron microscopy

Three adult guinea pigs were killed as described above. The eyecups were fixed in a mixture of 4% paraformaldehyde and 0.2% picric acid in PB for 30 min at room temperature. The retinas were then carefully dissected out; small pieces were taken from the central region and fixed for an additional 2 h at 4 °C. After washing in PB, the pieces were transferred to 30% sucrose in PB for 6 h at 4 °C, rapidly frozen in liquid nitrogen, thawed and embedded in 4% agar in distilled water. The retinal pieces were sectioned at 50 μm using a vibratome, and the sections were placed in PBS. They were incubated in 10% normal goat serum in PBS for 1 h at room temperature, to block non-specific binding, and then in Cx36 antibody diluted 1 : 1000 for 12 h at 4 °C.

The following immunocytochemical procedures were carried out at room temperature. The sections were washed in PBS for 45 min (3 × 15 min), incubated in biotin-labelled goat anti-rabbit IgG for 2 h, and then washed three times in PBS for 45 min (3 × 15 min). The sections were incubated in avidin–biotin–peroxidase complex (Vector Laboratories, Burlingame, CA, USA; diluted to 1 : 100) for 1 h, washed in TB, and then incubated in 0.05% 3,3′-DAB solution containing 0.01% H_2O_2. The reaction was monitored using a low-power microscope, and was stopped by replacing the DAB and H_2O_2 solution with TB.

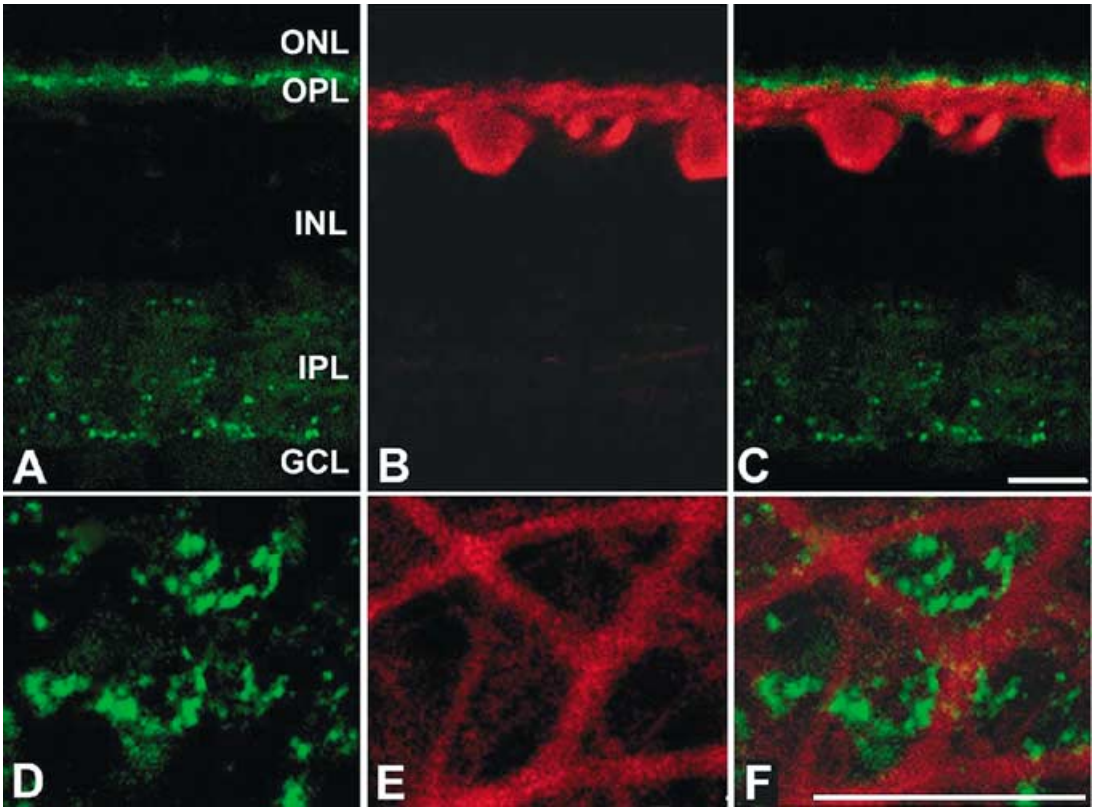

FIG. 2. Confocal micrographs taken from a vertical vibratome section (A–C) and a whole-mount preparation (D–F) processed for Cx36 (A and D) and calbindin (B and E) immunoreactivities. Cx36 immunoreactivity was visualized using an FITC-conjugated secondary antibody. Calbindin immunoreactivity was visualized using a Cy3-conjugated secondary antibody. (A) Cx36 immunoreactivity appears as discrete puncta, densely in the outer plexiform layer (OPL), in the ON sublamina of the inner plexiform layer (IPL), and sparsely in the OFF sublamina of the IPL. (B) A few calbindin-immunoreactive cell bodies are seen at the distal edge of the inner nuclear layer (INL). D and E focused at the OPL: Cx36-labelled puncta (D) and a calbindin-labelled network of horizontal cell processes (E) are seen. (C and F) Double-exposures of A, B, D and E show that Cx36-immunoreactive puncta are very close to the surface of the processes of horizontal cells, with no overlapping in staining. GCL, ganglion cell layer; ONL, outer nuclear layer. Scale bar, 50 μm.

The stained sections were post-fixed in 1% glutaraldehyde in PB for 1 h and, after washing in PB containing 4.5% sucrose for 15 min (3 × 5 min), they were then post-fixed in 1% OsO_4 in PB for 1 h. They were washed again in PB containing 4.5% sucrose, and dehydrated in a graded series of alcohol. During dehydration, they were stained *en bloc* with 1% uranyl acetate in 70% alcohol for 1 h, then infiltrated with propylene oxide and flat embedded in Epon 812. After the sections had been cured at 60 °C for 3 days, well-stained areas were cut out and attached to an Epon support for further ultrathin sectioning using a Reichert-Jung ultratome. Ultrathin sections (70–90 nm thick) were collected on one-hole grids coated with Formvar, and examined by transmission electron microscope (JEOL 1200EX, Tokyo, Japan).

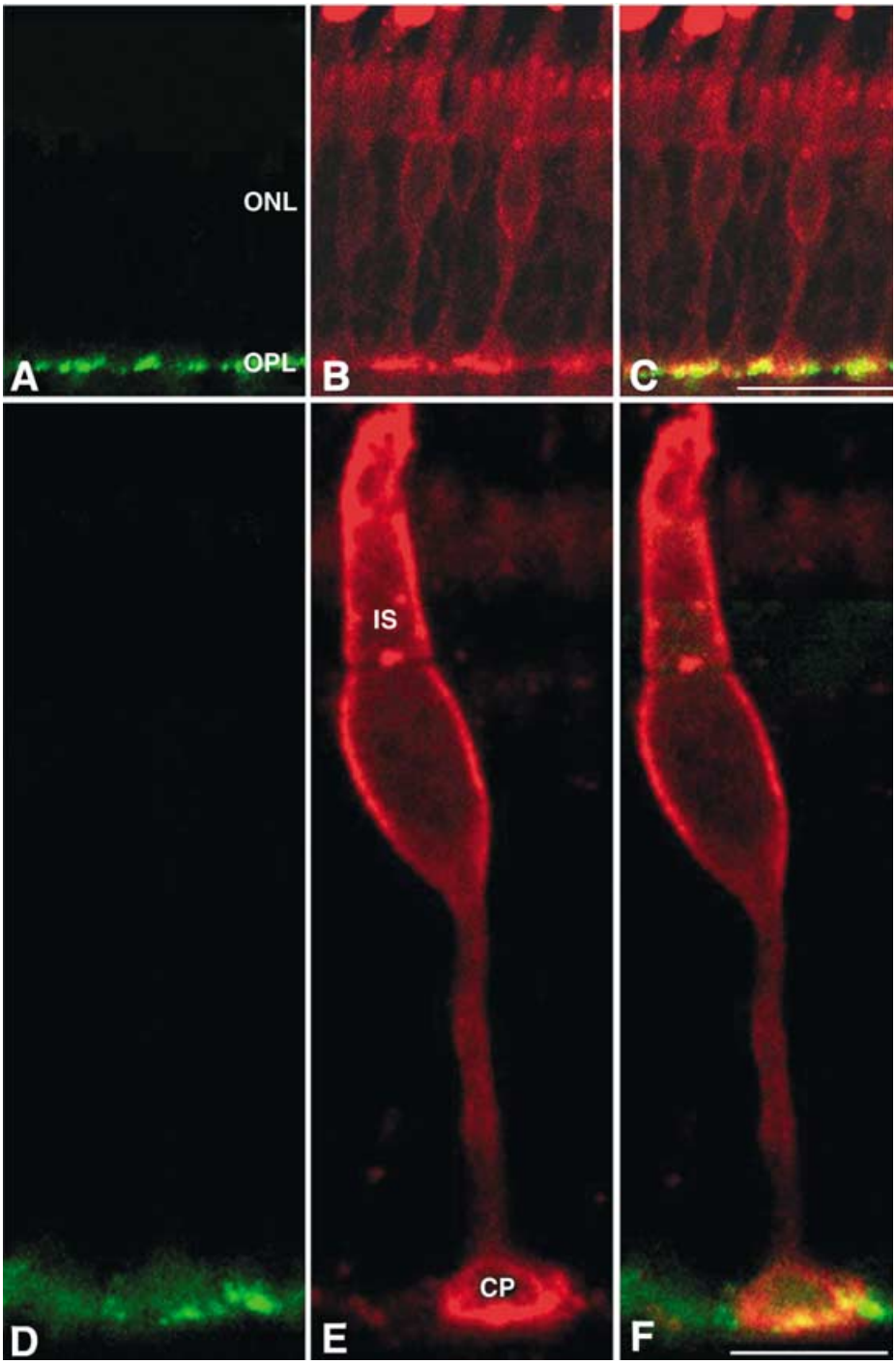

FIG. 3. Confocal micrographs taken from a vertical vibratome section processed for Cx35/36 (A) and green/red cone opsin (B) immunoreactivities. Cx35/36 immunoreactivity was visualized using an FITC-conjugated secondary antibody. Green/red cone opsin immunoreactivity was visualized using a Cy3-conjugated secondary antibody. (A) Cx35/36 immunoreactivity appears as discrete puncta in the OPL. (B) A few green/red cone opsin-immunoreactive cell bodies and terminals are visible. (D and E) Higher magnification micrographs of A and B, respectively. (C and F) Double exposures of A, B, D and E show that Cx35/36-immunoreactive puncta are concentrated at, and restricted to, the terminals of green/red cone pedicles (yellow). CP, cone pedicle; IS, inner segment; ONL, outer nuclear layer; OPL, outer plexiform layer. Scale bars, 50 μm (C); 10 μm (F).

Results

To test the specificity of the antibody, two sets of controls were run. In the first, Western blot analysis using an antibody against Cx36 or Cx35/36 was performed. In the second set, normal mouse or rabbit serum (pre-immune serum) was applied to the sections of the guinea pig retina. As shown in Fig. 1A, antibodies to Cx36 or Cx35/36 recognized a single band with a molecular mass of about 36 kDa in the retinal extracts. No immunostaining was visible in the section immunostained with pre-immune serum (Fig. 1B).

Cx36 or Cx35/36 immunoreactivity

Cx36- or Cx35/36-immunoreactive puncta were observed in the inner plexiform layer (IPL) and OPL in vertical sections of the guinea pig

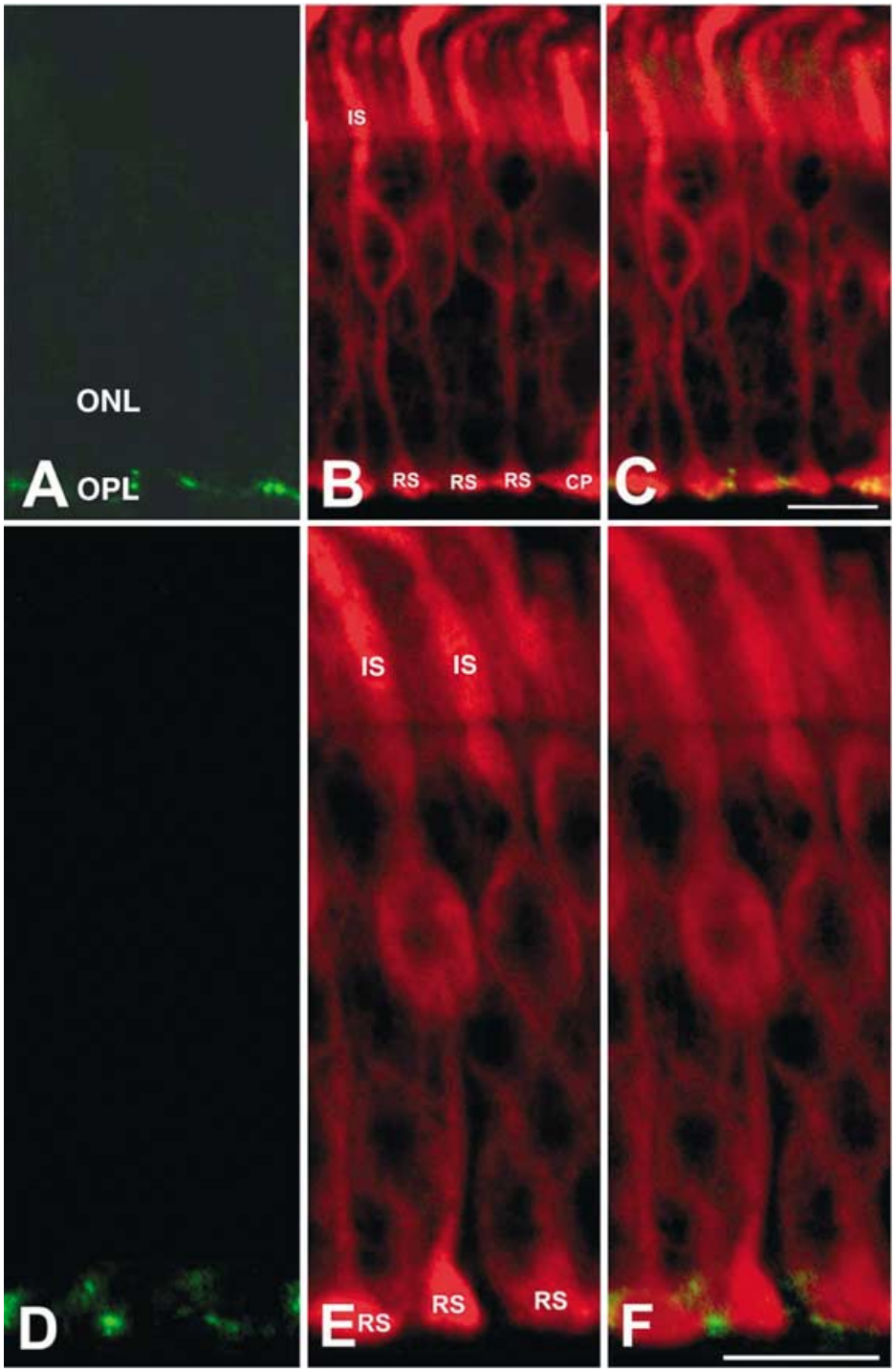

FIG. 4. Confocal micrographs taken from a vertical vibratome section processed for Cx35/36 (A) and recoverin (B) immunoreactivities. Cx36 immunoreactivity was visualized using an FITC-conjugated secondary antibody. Recoverin immunoreactivity was visualized using a Cy3-conjugated secondary antibody. (A) Cx35/36 immunoreactivity appears as discrete puncta in the outer plexiform layer (OPL). (B) A few recoverin-labelled rod and cone photoreceptor cells are visible. (D and E) Higher magnification micrographs of a vibratome section processed for Cx35/36 and recoverin immunoreactivities. (C and F) Double exposures of A and B. (D and E) Cx35/36-immunoreactive puncta are located adjacent to the rod spherule (RS). CP, cone pedicle; IS, inner segment; ONL, outer nuclear layer. Scale bars, 10 μm.

retina (Fig. 1C and D). The immunolabelling patterns of the Cx36 antibody (Fig. 1C) were quite similar to those of the Cx35/36 (Fig. 1D), except for faint non-specific Cx36 immunostaining in the outer segments of the photoreceptors. Although Cx36- or Cx35/36-immunoreactive puncta were visible throughout the whole depth of the IPL, they were more concentrated in the ON sublamina than the OFF sublamina of the IPL, as previously shown in the rat retina (Feigenspan *et al*., 2001).

Double-immunofluorescence for Cx36 and calbindin D-28k (calbindin)

A complex electrical coupling that forms a feedback mechanism to retinal photoreceptors exists between horizontal cells (Vaney & Weiler, 2000). To identify whether Cx36 is localized to gap junctions between horizontal cells, double-labelling experiments using antisera against Cx36 and calbindin were performed in vertical sections of the retina. An antiserum against calbindin is a specific marker for

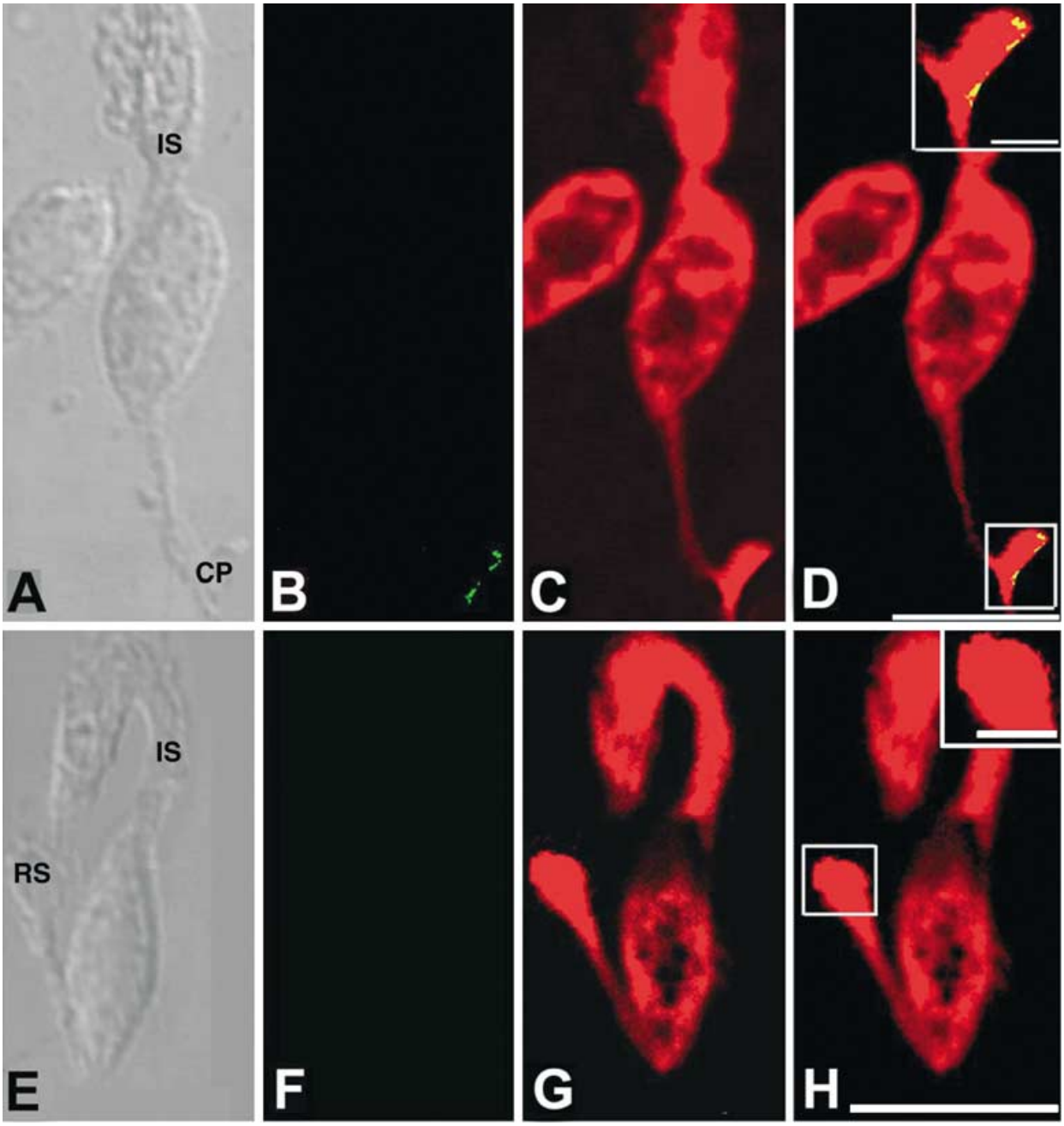

FIG. 5. (A and E) Light micrographs of dissociated cone (A) and rod (E) cells. Cone cells have wider inner segments (IS) and larger terminals (CP, cone pedicle) (A), whereas rod cells have thinner inner segments and smaller spherical terminals (RS, rod spherule) (E). Confocal micrographs taken from a cone cell (B–D) and a rod cell (F–H) processed for Cx35/36 (B and F) and for recoverin (C and G) immunoreactivities. Cx35/36 immunoreactivity was visualized using an FITC-conjugated secondary antibody. Recoverin immunoreactivity was visualized using a Cy3-conjugated secondary antibody. (B) Cx35/36-labelled small puncta are visible, whereas no labelled puncta are visible in F. Recoverin-labelled cone (C) and rod (G) cells are visible. (D and H) Double exposures of B, C, F and G show that Cx35/36-immunoreactive puncta are concentrated at the base of the cone pedicle (yellow), whereas no labelled puncta are visible in the rod spherule (H). Scale bars, 10 μm (D and H); 2.5 μm (rectangles).

horizontal cells in the mammalian retina (Röhrenbeck *et al*., 1987; Pochet *et al*., 1991; Uesugi *et al*., 1992). Figure 2 shows an example of a vertical section and a whole-mount preparation of the guinea pig retina, double-labelled with antibodies against Cx36 and calbindin. Calbindin immunoreactivity was found in the cell bodies and dendrites of horizontal cells near the OPL (Fig. 2B and E), and Cx36 immunoreactivity was observed in both the IPL and OPL (Fig. 2A and D). In a merged figure (Fig. 2C and F), horizontal cell processes are located just below the Cx36-immunoreactive puncta, and there is no overlap of the immunoreactivities. These results suggest that gap junctions between horizontal cells may not possess Cx36 in the guinea pig retina. However, dendrites and axon terminals of horizontal cells invaginating into the cone pedicles or rod spherules are not visible in the guinea pig retina, unlike those in other mammals. Thus, ultrastructural localization of Cx36-immunoreactive profiles was further confirmed by electron microscopy in the present study.

Localization of Cx35/36 at cone pedicles and rod spherules

Gap junctions between rods and cones have been identified (Raviola & Gilula, 1973), and functional rod–cone coupling has been reported in the primate retina (Schneeweis & Schnapf, 1995). In the alternative rod pathway, rod excitation could input directly to cone terminals and then be relayed to a subset of ganglion cells via ON and OFF cone bipolar cell circuitry (Smith *et al*., 1986). In the present study, double-labelling using antisera against Cx35/36 and green/red cone opsin or recoverin was performed to determine whether Cx35/36 is localized to cone pedicles and rod spherules (Figs 3–5). A monoclonal antibody opsin (Rho4D2) is known to specifically label the cell body, and outer segment, but not in their synaptic terminal in mammalian retina (Dorn *et al*., 1995; O'Brien *et al*., 2003). Therefore, we used antisera against recoverin, which is a much better marker for identifying rod terminals. The tissues were processed for immunocytochemistry using Cx35/36 (Fig. 3A and D) and green/red cone opsin (Fig. 3B and E) antibodies. Green/red cone opsin immunoreactivity was localized to an entire cone

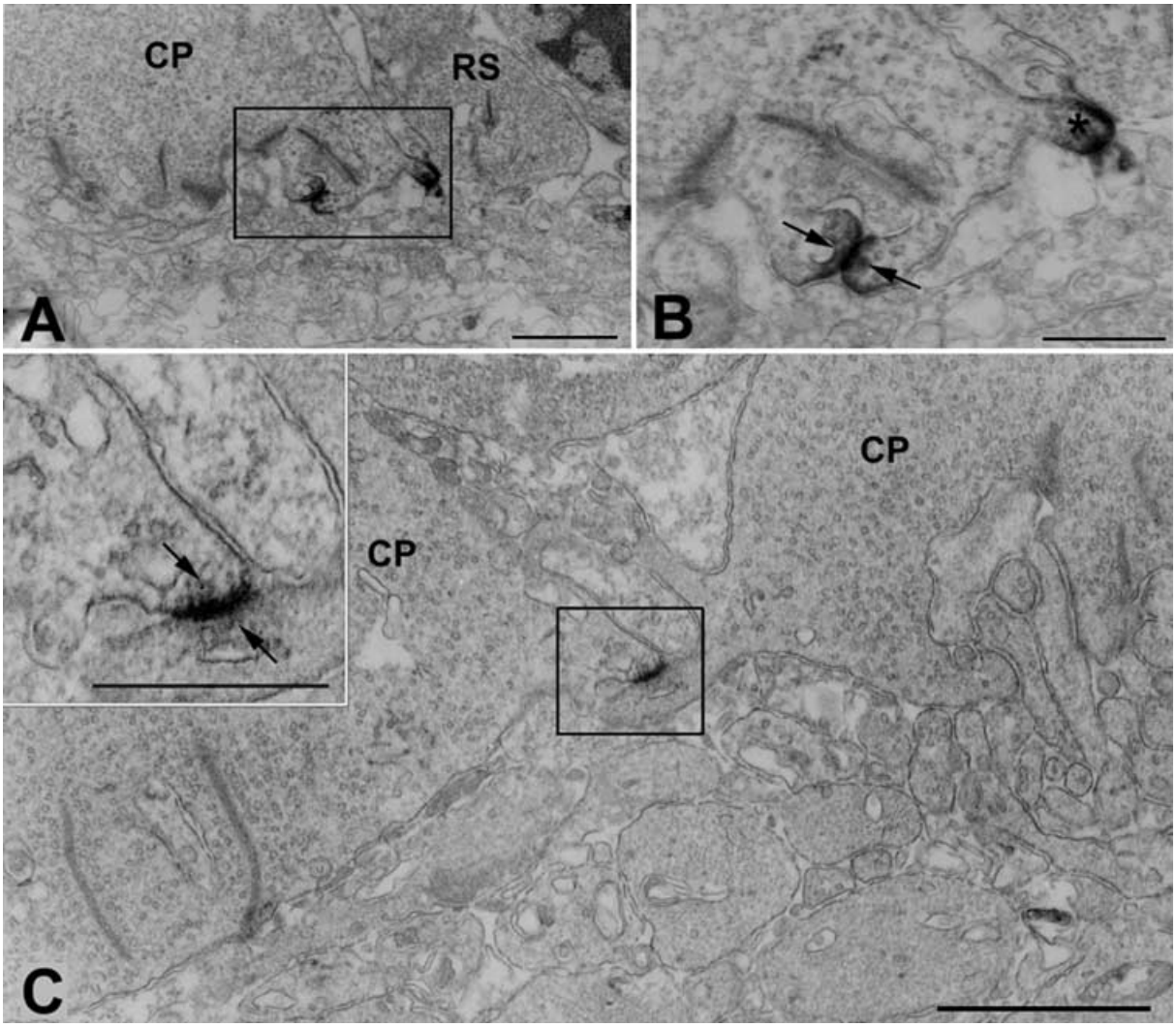

FIG. 6. Transmission electron micrographs showing vertical ultrathin sections of the OPL processed for Cx36 immunoreactivity. (A) Cx36 immunoreactivity is localized to the membrane or cytoplasmic matrices of the telodendria of a cone pedicle (CP). (B) A higher-magnification image indicated by the rectangle in A. Cx36 immunoreactivity is clearly visible at the gap junction and cytoplasmic matrices (arrows). A telodendrium indicated by asterisk shows Cx36 immunoreactivity, but this tip does not make gap junction with a neighbouring rod spherule (RS). (C) Cx36 immunoreactivity is localized to a gap junction between cone pedicles (CP). The inset rectangle shows a high-magnification view. Arrows indicate labelled gap junction and cytoplasmic matrices. Scale bars, 1 μm (A and C); 0.5 μm (B and in the inset).

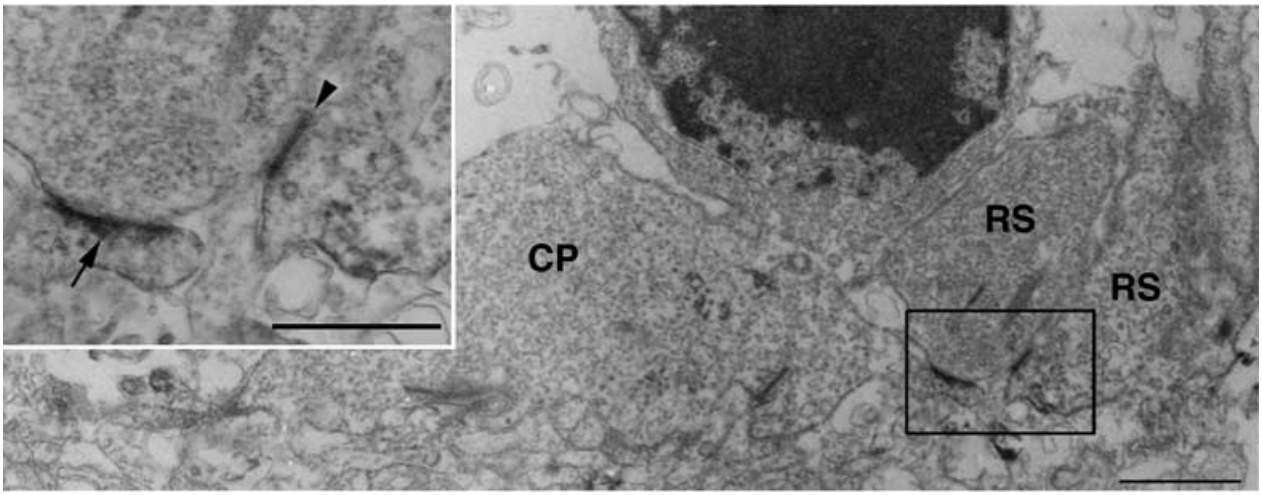

FIG. 7. Transmission electron micrographs showing vertical ultrathin sections of the OPL processed for Cx36 immunoreactivity. One cone pedicle (CP) and two rod spherules (RS) are visible. The inset rectangle shows a higher magnification view. Cx36 immunoreactivity is localized to cytoplasmic matrices close to the gap junction in a CP, whereas no immunoreactivity is visible in the cytoplasmic matrices of a RS. An arrowhead indicates a gap junction between RSs, in which no Cx36 immunoreactivity is visible. Scale bar, 1 μm; 0.5 μm (inset).

photoreceptor including a cone pedicle. In merged figures (Fig. 3C and F), it is apparent that the Cx35/36-immunoreactive puncta appear to be concentrated at and restricted to the green/red cone pedicles. A polyclonal antibody to recoverin labels all photoreceptors in the rat retina (Milam *et al*., 1993; Chun *et al*., 1999). Therefore, double-labelling using antisera against Cx35/36 and recoverin was performed to identify whether Cx35/36 is localized to the rod cells in the guinea pig retina (Fig. 4). Figure 4A was processed for Cx35/36 immunoreactivity, and Fig. 4B for recoverin immunoreactivity. Recoverin immunoreactivity was localized to all photoreceptors (Fig. 4B). In this figure, rod cells could be easily identified by their morphological features in that rod cells have a long outer segment, a thinner inner segment and a smaller spherical terminal than cone cells (Dowling, 1987). Higher magnified figures of different vibratome sections are shown as Fig. 4D–F. From this figure, rod cells are easily distinguishable by their morphological features. In a merged picture of Fig. 4A and B, Cx35/36-immunoreactive puncta appear to be close to rod spherules (Fig. 4C and F).

To examine the detailed distribution of Cx35/36 in the cone and rod cells, double-labelling using antisera against recoverin and Cx35/36 was performed on dissociated retinal cells. Figure 5 is an example of a dissociated cone cell (Fig. 5A) and a rod cell (Fig. 5E). Cone and rod cells were differentiated from their morphological features; cone cells have a fatter inner segment and a larger terminal than rod cells. Dissociated cone and rod cells were double-immunostained with antisera against Cx35/36 (Fig. 5B and F) and recoverin (Fig. 5C and G). In Fig. 5C and G, intact cone (Fig. 5C) and rod (Fig. 5G) cells showing recoverin immunoreactivity are clearly visible. In Fig. 5B, Cx35/36-immunoreactive puncta are seen closely aggregated as labelled clusters in the OPL of the vertical sections shown in Figs 3 and 4. With this double-labelling (Fig. 5D), it is apparent that Cx35/36 immunoreactivity is localized to the cone pedicle in the guinea pig retina. However, a merged picture (Fig. 5H) of Fig. 5F and G clearly shows that labelled puncta are not visible in the rod spherule.

Ultrastructural localization of Cx36

To identify the precise ultrastructural localization of Cx36 within the rod spherules and cone pedicles, we examined Cx36-immunoreactive profiles by transmission electron microscopy. Because Cx36 is a gap junction protein, we expected that Cx36 immunoreactivity would be localized to gap junctions. However, Cx36-like immunoreactivity was identified as an electron-dense reaction product that was closely associated with gap junctions as well as cytoplasmic matrices close to the gap junctions or cell membranes (Fig. 6). This discrepancy frequently occurred in ultrastructurally localizing γ-aminobutyric acid transporters and glutamate receptors, which are also known to be integral membrane proteins, using the same method in the present study (Ribak *et al*., 1996; Brandstätter & Hack, 2001). Thus, such a cytoplasmic localization could be attributed to pre-embedding immunocytochemical techniques using the ABC method. However, it cannot be excluded that some of the labelling represents proteins in transit to the gap junctions.

In Fig. 6A and B, the strong Cx36 immunoreactivity appears to be restricted to the gap junctions between telodendria of a cone pedicle as well as the cytoplasmic sides of both telodendria facing each other. In the right upper part of Fig. 6B, another tip of a cone pedicle showing strong Cx36 immunoreactivity is seen to be adjacent to a rod spherule. Figure 6C shows an example of a gap junction between cone pedicles. Reaction products are visible in the gap junction and in the cytoplasmic matrices close to the gap junction. Figure 7 shows an example of a gap junction between a cone pedicle and a rod spherule, and a gap junction between rod spherules. Reaction products are visible in the cytoplasmic matrices close to the cell membrane of a cone pedicle that makes a gap junction with a rod spherule. However, no reaction products are visible in the gap junction between rod spherules or in cytoplasmic matrices of rod spherules close to the gap junction. These results clearly demonstrate that cone pedicles make heterologous gap junctions containing Cx36 with nearby rod spherules.

Discussion

Here we investigated the expression and cellular localization of Cx36 in the guinea pig retina by immunocytochemistry and electron microscopy using antisera against Cx35/36 or Cx36. Cx35/36 or Cx36 immunoreactivity was visible in the IPL as sparsely distributed puncta, which were more concentrated in the ON sublamina. Cx35/36- or Cx36-immunoreactive puncta were also visible in the OPL where they were localized to the cytoplasmic matrices of cone pedicles that form gap junctions with other cone pedicles or with rod spherules. The immunostaining patterns of both antisera in the guinea pig retina were

identical. These results were expected because Cx36 shows a high sequence identity to Cx35, which is expressed at high levels in the skate retina (O'Brien *et al*., 1996).

The localization of Cx35/36 or Cx36 immunoreactivity in the IPL is in good agreement with investigations on other mammalian retinas (Feigenspan *et al*., 2001; Guldenagel *et al*., 2001; Mills *et al*., 2001), which have shown that Cx36 is predominantly expressed in a subclass of amacrine cells, the AII amacrine cells, in the ON sublamina. The labelled puncta in the IPL are responsible for homologous or heterologous coupling of AII cells or AII and ON cone bipolar cells, respectively (Mills *et al*., 2001). Thus, Cx36 is involved in the scotopic pathways in the IPL of the guinea pig retina as well as those of other mammals.

Cx35/36- or Cx36-immunoreactive puncta were visible here in the OPL of the guinea pig retina, as has also been shown in the rat retina by Feigenspan *et al*. (2001). However, in the OPL, the labelling was much more intense in the guinea pig retina than in the rat and mouse retina, in which few labelled puncta were visible (Feigenspan *et al*., 2001). Thus, cells in the outer retina make contacts via Cx36-containing junctions in both guinea pig and rat retinas, but the degree of contacts or the subtypes of connexins clearly vary between species. Horizontal cells form a large coupled network that feeds back to the photoreceptors (Weiler *et al*., 2000). Thus, to identify whether horizontal cells express Cx36 immunoreactivity, we performed double-labelling using antisera against Cx36 and calbindin. Strong calbindin immunoreactivity was localized to horizontal cell somata and their dendrites as shown in other mammals (Röhrenbeck *et al*., 1987, 1989; Pasteels *et al*., 1990; Peichl & González-Soriano, 1994). However, unlike other mammalian retina, labelled processes invaginating into the photoreceptor terminals were not clearly visible. This might be because the guinea pig retina contains more cones than other mammalian retina, or that axon terminals of B-type horizontal cells are not labelled by an antibody against calbindin. In the present double-labelling experiments, it cannot be excluded that horizontal cells express Cx36 immunoreactivity. However, we could not confirm this by electron microscopy. Therefore, it is apparent that calbindin-labelled horizontal cells do not express Cx36 immunoreactivity, as has also been shown in the mouse retina, in which horizontal cells do not express either Cx26 or Cx36 immunoreactivity (Deans & Paul, 2001). Thus, Cx36 is not involved in feedback inhibition or horizontal cell coupling (Janssen-Bienhold *et al*., 1998), and horizontal cells might contain other types of connexins.

Gap junctions play important roles in the visual processing in the retina by functioning as electrical synapses, which are dramatically modulated by neurotransmitters and the level of ambient illumination (Vaney, 1994; Cook & Becker, 1995; Sterling, 1995; Vaney, 1996; Baldridge *et al*., 1998). In addition to homologous electrical coupling between the same types of neurons, heterologous coupling also exists between cone cells and rod cells, between different types of amacrine cells, between different types of bipolar cells, and between ganglion cells and amacrine cells (Raviola & Gilula, 1973; Vaney, 1991, 1994; Vaney *et al*., 1998; Vaney & Weiler, 2000; Tsukamoto *et al*., 2001). The identity of all of the connexin proteins of gap junctions between photoreceptor cells of the mammalian retina is largely unknown, as there are only limited reports. Feigenspan *et al*. (2001) showed that Cx36-immunoreactive puncta are localized to the OPL of the rat and mouse retinas, and Deans *et al*. (2002) showed that the Cx36 coding sequence – replaced with a histological reporter sequence – is abundantly expressed in the OPL of the mouse retina. In the present study, Cx36 was at first identified as localized to the cone pedicles by double-labelling, and we confirmed that homologous gap junctions between cone pedicles and heterologous gap junctions between cone pedicles and rod spherules expressed Cx36 immunoreactivity using electron microscopy. In homologous gap junctions between cone cells, Cx36 immunoreactivity was visible in the gap junctions as well as in the cytoplasmic matrices of both sides, clearly indicating that Cx36 forms homotypic channels. In the heterologous gap junctions between cone pedicles and rod spherules, Cx36 immunoreactivity was localized to the gap junctions and to the cytoplasmic matrices of the cone pedicles. No Cx36 immunoreactivity was visible in the cytoplasmic matrices of the rod spherules. In addition, homologous gap junctions between rod spherules did not show any Cx36 immunoreactivity. Thus, heterologous junctions between cone cells and rod cells might be heterotypic channels composed of Cx36 in the cone cell sites and a different connexin type in the rod cell sites. Direct rod–cone coupling has been described in cold-blooded vertebrates (Schwartz, 1975; Yang & Wu, 1989; Krizaj *et al*., 1998), and rod signals within cone responses have been reported in cat (Nelson, 1977) and macaque retinas (Schneeweis & Schnapf, 1995). Both anatomical and functional data support the presence of rod–cone coupling in a variety of vertebrate retinas, including those of mammals (Raviola & Gilula, 1973; Nelson, 1977; Schneeweis & Schnapf, 1995), reptiles (Schwartz, 1975; Copenhagen & Owen, 1976) and amphibians (Gold & Dowling, 1979; Gold, 1979; Nagy & Witkovsky, 1981; Wu & Yang, 1988; Yang & Wu, 1989). Direct rod–cone coupling via gap junctions provides for rapid, sign-conserving signal transfers (Krizaj *et al*., 1998). In addition, rod signals might reach ganglion cells via a pathway independent of the rod bipolar cells and the AII amacrine cells. This alternative circuit involves gap junction coupling between rod and cone photoreceptors in the outer retina and is thought to subserve twilight vision (Raviola & Gilula, 1973; Kolb, 1977; Nelson, 1977; DeVries & Baylor, 1995; Schneeweis & Schnapf, 1995). Here, we have shown that the guinea pig retina provides alternative rod pathways, employing gap junctions between rods and cones. In this pathway, rod signals have access to ON and OFF cone bipolar cells, and then to ON and OFF ganglion cells (Nelson, 1977; Nelson & Kolb, 1983; Smith *et al*., 1986; Sterling & Lampson, 1986).

Acknowledgements

We are grateful to Dr J. Nathans at Johns Hopkins University School of Medicine for providing antisera against green/red cone opsin and to Dr L. Peichl at Max-Planck Institute for Brain Research for his valuable comments. This work was supported by the Korea Research Foundation (2000-FP0001) and BK 21 in Korea.

Abbreviations

calbindin, calbindin D-28k; Cx36, connexin 36; DAB, diaminobenzidine; FITC, fluorescein isothiocyanate; IPL, inner plexiform layer; OPL, outer plexiform layer; PB, phosphate buffer; PBS, phosphate-buffered saline; TB, tris buffer.

References

Baldridge, W.H., Vaney, D.I. & Weiler, R. (1998) The modulation of intercellular coupling in the retina. *Semin. Cell Dev. Biol.*, **9**, 311–318.

Beyer, E.C., Paul, D.L. & Goodenough, D.A. (1990) Connexin family of gap junction proteins. *Bioessays*, **18**, 709–718.

Brandstätter, J.H. & Hack, I. (2001) Localization of glutamate receptors at a complex synapse. The mammalian photoreceptor synapse. *Cell Tissue Res.*, **303**, 1–14.

Bruzzone, R., White, T.W. & Goodenough, D.A. (1996) The cellular Internet: on-line with connexins. *Cell Commun. Adhes.*, **8**, 361–366.

Chun, M.H., Kim, I.B., Oh, S.J. & Chung, J.W. (1999) Synaptic connectivity of two types of recoverin-labeled cone bipolar cells and glutamic acid decarboxylase immunoreactive amacrine cells in the inner plexiform layer of the rat retina. *Vis. Neurosci.*, **16**, 791–800.

Cook, J.E. & Becker, D.L. (1995) Gap junctions in the vertebrate retina. *Microsc. Res. Techn*, **31**, 408–419.

Copenhagen, D.R. & Owen, W.G. (1976) Functional characteristics of lateral interactions between rods in the retina of the snapping turtle. *J. Physiol. (Lond.)*, **259**, 251–282.

Dahl, E., Winterhager, E., Reuss, B., Traub, O., Butterweck, A. & Willecke, K. (1996) Expression of the gap junction proteins connexin31 and connexin43 correlates with communication compartments in extraembryonic tissues and in the gastrulating mouse embryo, respectively. *J. Cell Sci.*, **109**, 191–197.

Deans, M.R. & Paul, D.L. (2001) Mouse horizontal cells do not express connexin26 or connexin36. *Cell Commun. Adhes.*, **8**, 361–366.

Deans, M.R., Volgyi, B., Goodenough, D.A., Bloomfield, S.A. & Paul, D.L. (2002) Connexin 36 is essential for transmission of rod-mediated visual signals in the mammalian retina. *Neuron*, **36**, 703–712.

Dermietzel, R. & Spray, D.C. (1998) From neuro-glue ('Nervenkitt') to glia: a prologue. *Glia*, **24**, 1–7.

DeVries, S.H. & Baylor, D.A. (1995) An alternative pathway for signal flow from rod photoreceptors to ganglion cells in mammalian retina. *Proc. Natl. Acad. Sci. USA*, **92**, 10658–10662.

Dong, C.J. & McReynolds, J.S. (1991) The relationship between light, dopamine release and horizontal cell coupling in the mudpuppy retina. *J. Physiol. (Lond.)*, **440**, 291–309.

Dorn, E.M., Hendrickson, L. & Hendrickson, A.E. (1995) The appearance of rod opsin during monkey retinal development. *Invest. Ophthalmol. Vis. Sci.*, **36**, 2634–2651.

Dowling, J.E. (1987) *The Retina: an Approachable Part of the Brain*. Harvard University Press, London.

Feigenspan, A., Teubner, B., Willecke, K. & Weiler, R. (2001) Expression of neuronal connexin 36 in AII amacrine cells of the mammalian retina. *J. Neurosci.*, **21**, 230–239.

Galarreta, M. & Hestrin, S. (1999) A network of fast-spiking cells in the neocortex connected by electrical synapses. *Nature*, **402**, 72–75.

Gold, G.H. (1979) Photoreceptor coupling in retina of the toad, Bufo marinus. II. Physiology. *J. Neurophysiol.*, **42**, 311–328.

Gold, G.H. & Dowling, J.E. (1979) Photoreceptor coupling in retina of the toad, Bufo marinus. I. Anatomy. *J. Neurophysiol.*, **42**, 292–310.

Goodenough, D.A., Goliger, J.A. & Paul, D.L. (1996) Connexins, connexons, and intercellular communication. *Annu. Rev. Biochem.*, **65**, 475–502.

Guldenagel, M., Ammermuller, J., Feigenspan, A., Teubner, B., Degen, J., Sohl, G., Willecke, K. & Weiler, R. (2001) Visual transmission deficits in mice with targeted disruption of the gap junction gene connexin 36. *J. Neurosci.*, **21**, 6036–6044.

Haefliger, J.A., Bruzzone, R., Jenkins, N.A., Gilbert, D.J., Copeland, N.G. & Paul, D.L. (1992) Four novel members of the connexin family of gap junction proteins. Molecular cloning, expression, and chromosome mapping. *J. Biol. Chem.*, **267**, 2057–2064.

Janssen-Bienhold, U., Dermietzel, R. & Weiler, R. (1998) Distribution of connexin43 immunoreactivity in the retinas of different vertebrates. *J. Comp. Neurol.*, **396**, 310–321.

Kolb, H. (1977) The organization of the outer plexiform layer in the retina of the cat: electron microscopic observations. *J. Neurocytol.*, **6**, 131–153.

Krizaj, D., Gabriel, R., Owen, W.G. & Witkovsky, P. (1998) Dopamine D2 receptor-mediated modulation of rod-cone coupling in the Xenopus retina. *J. Comp. Neurol.*, **398**, 529–538.

Milam, A.H., Dacey, D.M. & Dizhoor, A.M. (1993) Recoverin immunoreactivity in mammalian cone bipolar cells. *Vis. Neurosci.*, **10**, 1–12.

Mills, S.L., O'Brien, J.J., Li, W., O'Brien, J. & Massey, S.C. (2001) Rod pathways in the mammalian retina use connexin 36. *J. Comp. Neurol.*, **436**, 336–350.

Nagy, A.R. & Witkovsky, P. (1981) A freeze-fracture study of synaptogenesis in the distal retina of larval Xenopus. *J. Neurocytol.*, **10**, 897–919.

Nelson, R. (1977) Cat cones have rod input: a comparison of the response properties of cones and horizontal cell bodies in the retina of the cat. *J. Comp. Neurol.*, **172**, 109–135.

Nelson, R. & Kolb, H. (1983) Synaptic patterns and response properties of bipolar and ganglion cells in the cat retina. *Vision Res.*, **23**, 1183–1195.

O'Brien, J., Al-Ubaidi, M.R. & Ripps, H. (1996) Connexin 35: a gap-junctional protein expressed preferentially in the skate retina. *Mol. Biol. Cell.*, **7**, 233–243.

O'Brien, KM., Schulte, D. & Hendrickson, AE. (2003) Expression of photoreceptor associated molecules during human fetal eye development. *Mol. Vis.*, **28**, 401–409.

Pasteels, B., Rogers, J., Blachier, F. & Pochet, R. (1990) Calbindin and calretinin localization in retina from different species. *Vis. Neurosci.*, **5**, 1–16.

Peichl, L. & González-Soriano, J. (1994) Morphological types of horizontal cell in rodent retinas: a comparison of rat, mouse, gerbil, and guinea pig. *Vis. Neurosci.*, **11**, 501–517.

Pochet, R., Pasteels, B., Seto-Ohshima, A., Bastianelli, E., Kitajima, S. & Van Eldik, L.J. (1991) Calmodulin and calbindin localization in retina from six vertebrate species. *J. Comp. Neurol.*, **314**, 750–762.

Raviola, E. & Gilula, N.B. (1973) Gap junctions between photoreceptor cells in the vertebrate retina. *Proc. Natl. Acad. Sci. USA*, **70**, 1677–1681.

Raviola, E. & Gilula, N.B. (1975) Intramembrane organization of specialized contacts in the outer plexiform layer of the retina. A freeze-fracture study in monkeys and rabbits. *J. Cell. Biol.*, **65**, 192–222.

Ribak, C.E., Tong, W.M. & Brecha, N.C. (1996) GABA plasma membrane transporters, GAT-1 and GAT-3, display different distributions in the rat hippocampus. *J. Comp. Neurol.*, **367**, 595–606.

Röhrenbeck, J., Wassle, H. & Boycott, B.B. (1989) Horizontal cells in the monkey retina: immunocytochemical staining with antibodies against calcium binding proteins. *Eur. J. Neurosci.*, **1**, 407–420.

Röhrenbeck, J., Wässle, H. & Heizmann, C.W. (1987) Immunocytochemical labelling of horizontal cells in mammalian retina using antibodies against calcium-binding proteins. *Neurosci. Lett.*, **77**, 255–260.

Schneeweis, D.M. & Schnapf, J.L. (1995) Photovoltage of rods and cones in the macaque retina. *Science*, **268**, 1053–1056.

Schwartz, E.A. (1975) Cones excite rods in the retina of the turtle. *J. Physiol. (Lond.)*, **246**, 639–651.

Smith, R.G., Freed, M.A. & Sterling, P. (1986) Microcircuitry of the dark-adapted cat retina: functional architecture of the rod-cone network. *J. Neurosci.*, **6**, 3505–3517.

Sterling, P. (1995) Vision. Tuning retinal circuits. *Nature*, **377**, 676–677.

Sterling, P. & Lampson, L.A. (1986) Molecular specificity of defined types of amacrine synapse in cat retina. *J. Neurosci.*, **6**, 1314–1324.

Tamas, G., Buhl, E.H., Lorincz, A. & Somogyi, P. (2000) Proximally targeted GABAergic synapses and gap junctions synchronize cortical interneurons. *Nature Neurosci.*, **3**, 366–371.

Traub, R.D., Schmitz, D., Jefferys, J.G. & Draguhn, A. (1999) High-frequency population oscillations are predicted to occur in hippocampal pyramidal neuronal networks interconnected by axoaxonal gap junctions. *Neuroscience*, **92**, 407–426.

Tsukamoto, Y., Morigiwa, K., Ueda, M. & Sterling, P. (2001) Microcircuits for night vision in mouse retina. *J. Neurosci.*, **21**, 8616–8623.

Uesugi, R., Yamada, M., Mizuguchi, M., Baimbridge, K.G. & Kim, S.U. (1992) Calbindin D-28k and parvalbumin immunohistochemistry in developing rat retina. *Exp. Eye Res.*, **54**, 491–499.

Umino, Y. & Saito, T. (2002) Spatial and temporal patterns of distribution of the gap junctional protein connexin43 during retinal regeneration of adult newt. *J. Comp. Neurol.*, **454**, 255–262.

Vaney, D.I. (1991) Many diverse types of retinal neurons show tracer coupling when injected with biocytin or Neurobiotin. *Neurosci. Lett.*, **125**, 187–190.

Vaney, D.I. (1994) Patterns of neuronal coupling in the retina. *Prog. Retinal Eye Res.*, **13**, 301–355.

Vaney, D.I. (1996) Cell coupling in the retina. In Spray, D.C. & Dermietzel, R. (Eds), *Gap Junctions in the Nervous System.* R.G. Austin, Landes, pp. 79–102.

Vaney, D.I. (1999) Neuronal coupling in the central nervous system: lessons from the retina. *Novartis Found. Symp.*, **219**, 113–125.

Vaney, D.I., Nelson, J.C. & Pow, D.V. (1998) Neurotransmitter coupling through gap junctions in the retina. *J. Neurosci.*, **18**, 10594–10602.

Vaney, D.I. & Weiler, R. (2000) Gap junctions in the eye: evidence for heteromeric, heterotypic and mixed-homotypic interactions. *Brain Res. Rev.*, **32**, 115–120.

Weiler, R. & Akopian, A. (1992) Effects of background illuminations on the receptive field size of horizontal cells in the turtle retina are mediated by dopamine. *Neurosci. Lett.*, **140**, 121–124.

Weiler, R., Pottek, M., He, S. & Vaney, D.I. (2000) Modulation of coupling between retinal horizontal cells by retinoic acid and endogenous dopamine. *Brain Res. Rev.*, **32**, 121–129.

Willecke, K., Hennemann, H., Dahl, E., Jungbluth, S. & Heynkes, R. (1991) The diversity of connexin genes encoding gap junctional proteins. *Eur. J. Cell Biol.*, **56**, 1–7.

Wu, S.M. & Yang, X.L. (1988) Electrical coupling between rods and cones in the tiger salamander retina. *Proc. Natl Acad. Sci. USA*, **85**, 275–278.

Yang, X.L. & Wu, S.M. (1989) Modulation of rod-cone coupling by light. *Science*, **244**, 352–354.

Zahs, K.R., Kofuji, P., Meier, C. & Dermietzel, R. (2003) Connexin immunoreactivity in glial cells of the rat retina. *J. Comp. Neurol.*, **455**, 531–546.